A Novel Cooperative Content Fetching-based Strategy to Increase the Quality of Video Delivery to Mobile Users in Wireless Networks

Shijie Jia, Changqiao Xu, *Member, IEEE*, Jianfeng Guan, Hongke Zhang and
Gabriel-Miro Muntean, *Member, IEEE*

Abstract—Cooperatively fetching video content with the help of other mobile nodes can release some of the pressure on storage and bandwidth of the constrained mobile devices in wireless networks and speeds up the localization process of video resources so as to support better quality of viewing experience. In this context, the discovery of the appropriate mobile cooperative node becomes a key factor and is also a challenge for the deployment of such a fetching scheme. In this paper, we introduce a novel cooperative content fetching-based strategy to increase the quality of video delivery to mobile users in wireless networks (CCF). By intelligently monitoring the real-time variation in the state of the one-hop neighbors (immediate-neighbors) of the video resource downloader, CCF employs an innovative estimation model to measure the stability of these immediate-neighbors. In order to enhance the cooperative fetching efficiency, CCF designs a communication quality forecast model to measure link reliability and forecast the available bandwidth. By making use of a newly proposed cooperative fetching algorithm, CCF can speed up fetching and disseminating of video resources with the help of cooperative neighbors selected in terms of stability and communication quality. Simulation results show how CCF obtains higher selection accuracy of cooperative neighbors, lower average end-to-end delay, lower average packet loss ratio, higher average throughput, higher video quality and lower maintenance overhead in comparison with state of the art solutions.

Index Terms—Stability, Video Delivery, Cooperative Fetching, Wireless Networks, Video Quality.

I. INTRODUCTION

THE latest developments in mobile and wireless networks have fueled an impressive growth in type and number of

S. Jia is with the State Key Laboratory of Networking and Switching Technology, Beijing University of Posts and Telecommunications, Beijing 100876, China. He is also with the Academy of Information Technology, Luoyang Normal University, Luoyang 471022, Henan, China (e-mail: shjjia@gmail.com).

C. Xu and J. Guan are with the State Key Laboratory of Networking and Switching Technology, Beijing University of Posts and Telecommunications, Beijing 100876, China (e-mail: {cqxu,jfguan}@bupt.edu.cn).

H. Zhang is with the National Engineering Laboratory for Next Generation Internet Interconnection Devices, Beijing Jiaotong University, Beijing 100044, China (e-mail: hkzhang@bupt.edu.cn).

G.-M. Muntean is with the Performance Engineering Laboratory, School of Electronic Engineering, Network Innovations Centre, Rince Institute, Dublin City University, Dublin 9, Ireland (e-mail: gabriel.muntean@dcu.ie).
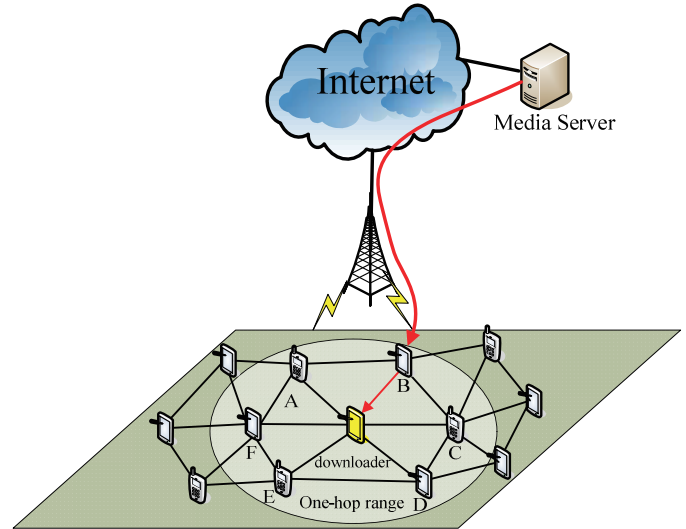
Fig. 1. Example of one-hop neighbor cooperative fetching

applications in commercial, entertainment, military, and educational areas [1]. Among these, providing rich media content to mobile users is increasingly popular and was responsible for over one-third of all consumer network traffic [2]-[5]. New multimedia applications like 3D stereo video have become the irreversible trend and trigger higher bandwidth demand than traditional streaming service [6]-[9]. However, supporting efficient high quality real-time video delivery to mobile users in wireless networks is very challenging mostly due to mobile device and network constraints in terms of bandwidth, storage and link reliability, especially in wireless multi-hop environments [10]-[13]. Unfortunately, user perceived quality for multimedia services delivered over these networks is in general low.

Recently, cooperation has become the underlying guiding principle in numerous (media) resource fetching research efforts [14]-[24]. For instance, information-centric networking (ICN) is a clean-slate networking architecture that puts information in focus instead of the interconnection of specific nodes so as to achieve efficient and reliable distribution of resources [25]. ICN architectures leverage in-network collaborative storage for caching, multiparty communication through replication and interaction models in terms of interest and distribution for resources. ICN accelerates the dissemination

and sharing of resources and helps where there is shortage of available resources. However, none of these approaches involving management, retrieval and distribution of video resources can support real-time multimedia streaming service in mobile wireless networks. Moreover, the churn for replacing resources results in wasting the bandwidth and storage and increasing the energy consumption of the mobile nodes.

Making cooperative use of the storage space and bandwidth of the nodes geographically close to the downloader (e.g. one-hop neighbors) to fetch media resources, not only meets the real-time requirements of media streaming services, but also speeds up the download process, improves resource sharing capacity and overcomes the negative influence of the frequent link breaks in wireless multi-hop communications. A number of proposals have exploited the benefit of cooperation among mobile nodes which have close geographical location [14][19][22][24]. The performance of the cooperation mode relies on the selection of cooperative nodes. The mobility of mobile nodes leads to dynamic variation of geographical location and communication quality between the two cooperative parties, reducing the efficiency of media resource delivery. However, there are some deficiencies in the selection of the cooperative nodes in the existing studies. For instance, some related resource sharing algorithms rely on the supposition that the cooperative parties have close geographical location during a certain period time [14] or neglect the mobility of mobile nodes [22]. Therefore, an efficient solution based on sensing mobility variation of mobile nodes and communication quality in the transmission path of media content should be considered for cooperative fetching strategies in wireless networks.

In this paper, we propose a novel ***Cooperative Content Fetching-based strategy to increase the quality of video delivery to mobile users in wireless networks*** (CCF). As Fig. 1 shows, the path of cooperative fetching video content includes two parts: from the downloader to the cooperative node (CN) (i.e. from the downloader to node B) and from the cooperative node to the content supplier (i.e. from node B to the server). CCF relies on an innovative stability estimation model (SEM) and a novel communication quality forecast model (CQFM) to select the cooperative node from one-hop neighbors and improve the performance of cooperative fetching of video content. SEM evaluates the mobility stability of the one-hop neighbors in terms of the mobility volatility, in order to keep a stable one-hop neighbor relationship between the downloader and selected CN and obtain high transmission efficiency in the path from the downloader to CN. CQFM measures link reliability and forecasts available bandwidth of the one-hop neighbors in the whole path of cooperative fetching, which enhances the delivery capacity of video data. For each downloader, CCF considers the one-hop neighbor which has the more stable one-hop neighbor relationship with the downloader and the higher and more reliable forecasted bandwidth as a CN, which ensures the efficiency of cooperative fetching. CN-assisted fetching algorithm shortens the process of video resource localization and avoids the use of multi-hop links in order to increase the quality of viewing experience. Extensive tests show how CCF achieves much better performance results in comparison with other state of the art solutions.

II. RELATED WORKS

There have been numerous recent studies on cooperative fetching. *Tu et al.* proposed a collaborative content fetching scheme for groups of mobile subscribers with common characteristics (*C5*) [14]. *C5* makes use of a small scale P2SP framework in a hybrid mobile network to maximize the utility of WWAN links in order to cope with concurrent mobile Internet traffic. The nodes in close vicinity which use the high-speed WLAN form a group whose members share their own data with other requesting members by making use of multicast at MAC layer. $C5$ can speed up the fetching rate for community members by using idle WLAN interfaces for in-community communication. However, $C5$ relies on the premise that a number of mobile subscribers are close to each other for a period of time and fetch the same content from Internet, which is not true most of the time. In MobTorrent [15], individual vehicles use the WWAN radio (e.g. GPRS) to inform one (or multiple) selected AP(s) to pre-fetch content. The pre-fetched data is then replicated to other carrier nodes (mobile helpers) and propagated to the requesting vehicle. By making use of cooperative pre-fetching, the vehicle breaks the constraints of the bandwidth to download large-size files in short periods of time. However, MobTorrent depends on a necessary premise: mobility information of vehicles can be predicted with high accuracy using the Automatic Vehicle Location (AVL) system and past history, which is not always the case. *Cruces et al.* proposed a carrier selection strategy based on contact maps and has deployed his solution in a vehicular space [18]. By analyzing historical data of inter-vehicle communication, contact maps among vehicles are built. Contact maps can be exploited by APs in the cooperative download process, by estimating the meeting probability between downloader and candidate data carriers in order to select most promising local vehicles as data carriers. However, by making use of AP-to-AP and AP-to-vehicle information exchange to estimate the meeting probability of two vehicles, the overhead of information exchange, startup delay and probability of failure in the carrier selection strategy increase and consequently the solution will not meet the real-time demands of media streaming services. *Malandrino et al.* proposed a solution to enhance the AP deployment to optimize the performance of vehicular cooperative download in urban scenarios, by addressing channel contention and data transfer paradigm [20]. However, the solution needs to have perfect knowledge of vehicle trajectories and schedule of data transmissions. Furthermore, the multi-hop traffic delivery between the downloader and cooperative node (other vehicle or AP) is subjected to long delays and frequent link breaks.

Raveendran et al. proposed a mobile multipath cooperative network for real-time multimedia services [19]. A mobile device can access the cloud using multiple access links provided by its neighboring mobile devices. By dynamically establishing multiple paths among neighboring cooperative devices over WWAN and WLAN, the provider of video resources uses the distinct end-to-end paths to deliver the streaming data

to the requester. The combined capacity of multiple wireless access links enable support for higher throughput so as to guarantee increased user perceived quality for the multimedia service. However, this solution neglects the investigation of mobility for neighboring cooperative devices. The movement of cooperative devices leads to the unstable links and declining quality levels for the multimedia content delivery, so the performance of multipath transmission is negatively influenced. PatchPeer proposed in [22] uses a "Closest Peer" scheme to select the patching peer with the closest Euclidean distance from its one-hop neighbors to receive patch media streaming data. The patch streaming service provided by the closest peer supports continuous high quality service provisioning with low delay and reduced packet loss ratio (PLR). However, PatchPeer neglects the fact that the node mobility incurs and the distance between the initial closest peer and requester changes in time. If the closest peer becomes a multi-hop neighbor instead of a one-hop neighbor, the quality of the media streaming service quickly declines.

Ahlgren et al. proposed a cooperative caching approach in mobile ad-hoc networks (COCA) [23]. COCA groups the mobile nodes in MANETs into several clusters where the members in clusters have specified roles and autonomously maintain the cluster structure. The mobile nodes implement cooperative caching in the process of forwarding data and flexibly manage the cached content (e.g. removing obsolete content and caching new data). COCA uses a hierarchical searching strategy to disseminate the resource request messages according to the priority sequence: local, neighbors and data center. COCA takes full advantage of the storage space of each mobile node to increase the efficiency of resource searching in mobile ad-hoc networks. However, the cluster head needs to respond the request message and maintain the cluster members. The cluster head cannot support the high load due to the capacity constraints of the mobile device in terms of storage, computing and energy. The caching and replacement of data can further consume the limited energy. Therefore, COCA is difficult to adapt to the mobile environment. Moreover, the proposed request dissemination algorithm relies on message broadcast, which increases the network load, wastes network bandwidth and involves high delays. *Hao et al.* proposed a secure cooperative data downloading framework for paid services in vehicular ad hoc networks [24]. The vehicles make use of a coordination channel to broadcast one-hop request messages. The neighbor nodes of requester forward the request message to a road side unit (RSU). After receiving the request message, several vehicles which have relative close geographical distance with the requester are assigned to download the specified data unit from RSU and forward it to the requester. The cooperative download approach can facilitate data downloading and avoid the hidden terminal issue by coordinating the relay transmission. However, the proposed solution focuses on non-real time data downloading in a highway scenario only. The complex mobility of vehicles brings negative effects on the efficiency of downloading and sharing of data in a non-linear urban environment. Moreover, the high coordination complexity between multiple cooperative nodes cannot ensure real-time delivery of data.

The stability of the one-hop neighbor relationship between downloader and cooperative node and the of communication quality level play the important role in cooperative fetching algorithm. This is due to the fact that they have a direct effect on viewer perceived quality.

III. CCF Detailed Design

For convenience, Table I defines several notations which are used in this section and the following ones. Assume each mobile device is equipped with a GPS receiver, a wireless network interface and a video player. As illustrated in Fig. 1, the wireless signal range of each mobile node N_i (potential "downloader"), defines its *Immediate Neighbor Region (IN-R)*, similar to [26]. Each mobile node n_j, one-hop neighbor in N_i's INR (e.g., A, B, C, D, E and F) is considered N_i's *immediate-neighbor (IN)* [27]. By making use of GPS receiver-based "location-awareness" as described in [26][28], N_i can obtain the geographic position of all its IN nodes in INR. N_i's wireless network interface supports the transmission of multimedia data and exchanges control messages between N_i and its IN nodes. N_i makes use of one-hop multicast at MAC layer to detect the state of each of its IN nodes. These IN nodes respond with messages containing their average moving speed.

N_i uses a list to store the information related to its IN nodes, as follows: $NL_i \Leftrightarrow (n_1, n_2, ..., n_n)$ is the IN list of N_i, where $n_c \Leftrightarrow ((X_c, Y_c), sp_c)$ is a 2-tuple containing the coordinates of the geographic position and the average moving speed of node n_c, IN of N_i, listed in NL_i. Along with the movement of mobile nodes, the relationship between the geographic positions of the IN nodes dynamically changes, and therefore the membership of NL_i set varies. By reusing the "location-awareness" approach and sending the detection message at regular time intervals, N_i obtains new IN set data $NL_i^{(new)} \Leftrightarrow (n_1, n_2, ..., n_m)$. All items in the finite set $S = (NL_i^{(new)} \cap NL_i) = (n_a, n_b, ..., n_v)$ are considered as CN candidates, where the length of S is v.

N_i manages the IN nodes in terms of their joining, leaving or staying in the INR. If an IN node n_j leaves/enters N_i's INR, N_i removes/adds n_j's information from/to NL_i. In order to discover CN from the IN nodes, N_i assesses the mobility stability in INR and communication quality of all items of S according to CCF's SEM and CQFM algorithms. Consequently, CCF can be considered as a self-aware cognitive loop process [29], as illustrated in Fig. 2.

(1) *SEM: mobility stability estimation of IN nodes*. For all the items in S, N_i investigates node mobility based on the spatial distance and average moving speed relative to N_i (the relative distance and moving speed of IN nodes from N_i are considered as estimation parameters of *movement state of IN nodes*). N_i estimates the mobility volatility of all the items in S in current and previous update rounds in order to be aware of the variation levels of movement state of the IN nodes (*sensing mobility volatility of INs*). N_i dynamically regulates the period time of updating the IN nodes in terms of estimated mobility volatility (*calculate update period time*). The update period time is used to obtain the statistical information of

time spent in N_i's INR (expressed in seconds) which is a key parameter for the estimation of mobility stability of the IN nodes. N_i uses the movement direction and variation level of spatial distance and average moving speed from N_i of each item in S to calculate the weighted time spent in N_i's INR. These values are considered node's stability values (***estimate stability of INs***).

TABLE I
NOTATIONS USED BY CCF

| Notations	Descriptions
N_i	a mobile node i in a wireless network
NL_i	IN list of N_i
sp_c	average moving speed of mobile node n_c
$NL_i^{(new)}$	updated IN list of N_i
S	intersection of NL_i and $NL_i^{(new)}$
v	length of S
n_j	a IN of N_i
$G(N_i)$	estimate value of mobility volatility of INs in N_i
$E(S^{(c)})$	mobility estimate value of INs in the current update round
$I(S^{(p)})$	mobility estimate value of INs in the previous update round
$n_j^{sd_{ij}}$	spatial distance between n_j and N_i
$n_j^{\lvert sp_{ij}\rvert}$	relative average moving speed between n_j and N_i
$D(S^{(c)})$	distribution of relative average moving speed and spatial distance between INs and N_i
$r^{D(S^{(c)})}$	correlation coefficient of movement state of INs in N_i
$d_{N_i \to l}^{D(S^{(c)})}$	vertical distance from origin mapped by N_i to fitting line generated by $D(S^{(c)})$ in plane of relative average moving speed and spatial distance
b_l	slope of fitting line of $D(S^{(c)})$'s linear regression
ut_i	duration of the next update round of N_i
$ut^{(P)}_i$	duration of the current update round of N_i
R_i	proportion of sample size of mobility stability estimation
DR_{ij}	angle cosine of movement vector of N_i and n_j
st_{ij}	estimate value of n_j's stability in the current update round
$st_{ij}^{(P)}$	estimate value of n_j's stability in the previous update round
INS_i	N_i's IN subset whose items have a stability value greater than 0
$B_{jx}^{(O)}(t_k)$	estimate value of bandwidth between n_j and n_x in t_k
$AB_{jx}^{(O)}$	original series of bandwidth between n_j and n_x
$B_{jx}^{(A)}(t_k)$	accumulated value of bandwidth between n_j and n_x in t_k
$AB_{jx}^{(A)}$	accumulated series of bandwidth between n_j and n_x
a	Grey level of development
u	Grey level of control
$C_{jx}(v)$	residual value between $B_{jx}^{(O)}(t_v)$ and $\hat{B}_{jx}(v)$
$\bar{C}_{jx}$	residual mean value
F_{jx}	residual variance
$R_{jx}^{(P)}$	posteriori variance ratio
$TH^{(R)}$	a threshold value for measuring $R_{jx}^{(P)}$
$TH^{(P)}$	a threshold value for measuring $P_{jx}^{(P)}$
INX_i	N_i's IN subset whose items have reliable link state in the path from the IN nodes to video content supplier
INI_i	N_i's IN subset whose items have reliable link state in the path from the IN nodes to N_i
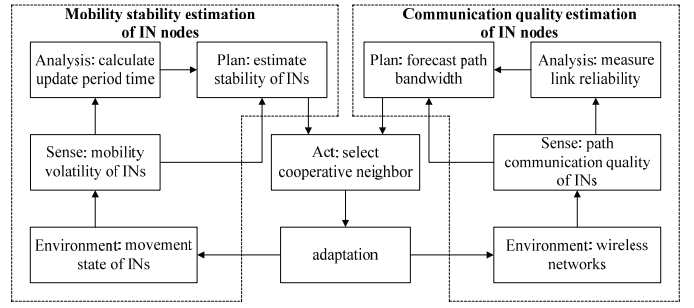
Fig. 2. The cognitive loop of CCF

(2) ***CQFM: communication quality estimation of IN nodes***. N_i investigates the bandwidth of the video delivery path for all the items in S. The delivery path from the supplier of video resources to N_i is divided into two parts: N_i to CN and CN to supplier. N_i selects its relatively high stability IN nodes to estimate the communication quality (i.e. link reliability and bandwidth forecasting value) in their paths of cooperative fetching (***path communication quality of INs***). N_i filters the IN nodes with unreliable links (***measure link reliability***) and forecasts the bandwidth of the video delivery path of the IN nodes with reliable links (***forecast path bandwidth***).

N_i selects an IN node with both relatively high stability and good communication quality in the video delivery path as the CN to help fetch the video resources (***select cooperative neighbor***). Once the CN contacts the supplier and receives the video streaming data, the data is forwarded to N_i. Therefore, CCF adapts to the dynamic environment by estimating the mobility and communication quality of IN nodes (***adaptation***). In order to best design SEM and CQFM, CCF needs to address the following four key problems:

(1) ***immediate neighbors' volatility estimation***. The nodes in S are considered stable IN nodes, as they have experienced one or multiple update period(s) of N_i. We investigate node mobility level based on the volatility of spatial distance and average moving speed relative to N_i for all items in S.

(2) ***IN list membership update***. CCF employs a variable update period scheme to implement the maintenance of the IN lists. In terms of IN nodes' volatility estimation, N_i can timely adjust the update period.

(3) ***weight-based membership stability estimation***. The influence of node mobility on stability estimation is considered. Variations of speed, direction and spatial distance from N_i for each IN node in S are used as weight factors to calculate the stability value of mobility.

(4) ***communication quality forecast***. The selected IN nodes periodically measure the available bandwidth to supplier. By investigating the variation level of the bandwidth, N_i estimates link reliability and forecasts the available bandwidth for these IN nodes.

A. Immediate Neighbors' Volatility

The motivation for the estimation of any node N_i's ***Immediate Neighbors' Volatility*** is to discover the variation level of mobility for all IN nodes in S in order to influence the update

period for the IN list. Inspired by the Information Theory model [30], we use the information content $G(N_i)$ to indicate the mobility variation as in eq. (1).

$$G(N_i) = E(S^{(c)}) - I(S^{(p)}), \; G(N_i) \in [-1, 1] \quad (1)$$

where $S^{(c)}$ and $S^{(p)}$ are the current and previous mobility of IN nodes in S for the update period at N_i, respectively. $E(S^{(c)})$ and $I(S^{(p)})$ are information entropy generated by $S^{(c)}$ and $S^{(p)}$, respectively and their values are obtained from eq. (2) and eq. (12), respectively.

$$E(S^{(c)}) = \begin{cases} -P^{(c)}\log_2 P^{(c)} & 0 < P^{(c)} < 1 \\ 0 & P^{(c)} = 0 \\ 1 & P^{(c)} = 1 \end{cases} \quad (2)$$

$P^{(c)}$ indicates the estimation value for mobility of all items in $S^{(c)}$. By investigating the mobility distribution of all items in $S^{(c)}$, we use the Least Square Method (LSM) [31] and the Linear Regression Fitting (LRF) [32] to calculate $P^{(c)}$. Let $D(S^{(c)})$ be the finite set denoting the distribution of mobility where each item composed of 2-tuples stores the average moving speed and spatial distance relative to N_i for each IN item in $S^{(c)}$, according to eq. (3).

$$D(S^{(c)}) = \{(n_a^{sd_{ia}}, n_a^{|sp_{ia}|}), (n_b^{sd_{ib}}, n_b^{|sp_{ib}|}), ..., (n_k^{sd_{ik}}, n_k^{|sp_{ik}|})\} \quad (3)$$

where $n_j^{sd_{ij}}$ and $n_j^{|sp_{ij}|}$ are the spatial distance and average moving speed relative to N_i of IN node $n_j \in S$ respectively. $n_j^{sd_{ij}}$'s initial value can be obtained from eq. (4).

$$n_j^{sd_{ij}} = \sqrt{(X_i - X_j)^2 + (Y_i - Y_j)^2}, \; n_j^{sd_{ij}} \in [0, n_{MAX}^{sd}] \quad (4)$$

where (X_i, Y_i) and (X_j, Y_j) are the geographic position coordinates of N_i and n_j, respectively. n_{MAX}^{sd} is the maximum distance from N_i and its value should be set to the radius R of INR (expressed in meters (m)). $n_j^{|sp_{ij}|}$'s initial value derives from the absolute value of the difference between the average moving speed of N_i and n_j, according to eq. (5).

$$n_j^{|sp_{ij}|} = \begin{cases} |N_i^{sp} - n_j^{sp}| & 0 \leq |N_i^{sp} - n_j^{sp}| < n_{MAX}^{sp} \\ n_{MAX}^{sp} & |N_i^{sp} - n_j^{sp}| \geq n_{MAX}^{sp} \end{cases} \quad (5)$$

In eq. (5) N_i^{sp} and n_j^{sp} are the average moving speeds of N_i and n_j, respectively and n_{MAX}^{sp} is the maximum value of the relative moving speed defined by CCF (expressed in m/s). For convenience, each item in $D(S^{(c)})$ needs to be normalized as indicated in eq. (6).

$$\hat{n}_j^{|sp_{ij}|} = \frac{n_j^{|sp_{ij}|}}{n_{MAX}^{sp}}, \; \hat{n}_j^{sd_{ij}} = \frac{n_j^{sd_{ij}}}{n_{MAX}^{sd}}, \; \hat{n}_j^{|sp_{ij}|}, \hat{n}_j^{sd_{ij}} \in [0, 1] \quad (6)$$

Assume N_i is the origin point of a coordinate system in which abscissa x and ordinate y represent the distance from N_i and the average moving speed relative to N_i, respectively, as shown in Fig. 3. The items in the $D(S^{(c)})$ set can be mapped
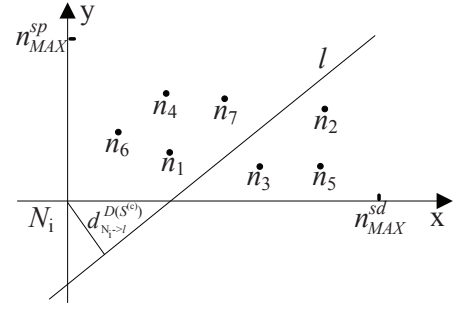

Fig. 3. Linear regression fitting model

into this coordinate system. l is the linear regression fitting line for $D(S^{(c)})$ and $d_{N_i \to l}^{D(S^{(c)})}$ is the vertical distance from origin to the fitting line. We use LSM to calculate the correlation coefficient $r^{D(S^{(c)})}$ and consider $d_{N_i \to l}^{D(S^{(c)})}$ and $r^{D(S^{(c)})}$ as estimation parameters for calculating $P^{(c)}$ according to eq. (7).

$$P^{(c)} = r^{D(S^{(c)})} \times (1 - d_{N_i \to l}^{D(S^{(c)})}), \quad P^{(c)} \in [0, 1] \quad (7)$$

In eq. (7) $r^{D(S^{(c)})} \in [0, 1]$ is the correlation coefficient of the regression data point in $D(S^{(c)})$ which indicates the difference level of the mobility (relative spatial distance and average moving speed) of all items in $S^{(c)}$, according to eq. (8). The larger the value of $r^{D(S^{(c)})}$ is, the lower the mobility state difference of all items in $S^{(c)}$ is.

$$r^{D(S^{(c)})} = \frac{\sum_{c=1}^{k} |\hat{n}_c^{|sp_{ic}|} - \overline{\hat{n}^{sp}}| \times |\hat{n}_c^{sd_{ic}} - \overline{\hat{n}^{sd}}|}{\sqrt{\sum_{c=1}^{k} |\hat{n}_c^{|sp_{ic}|} - \overline{\hat{n}^{sp}}|^2} \times \sqrt{\sum_{c=1}^{k} |\hat{n}_c^{sd_{ic}} - \overline{\hat{n}^{sd}}|^2}} \quad (8)$$

where $\overline{\hat{n}^{sp}}$ and $\overline{\hat{n}^{sd}}$ are the mean value of the average moving speed relative to N_i and the distance from N_i of all items in $S^{(c)}$, respectively. Their values can be obtained according to eq. (9).

$$\overline{\hat{n}^{sp}} = \frac{\sum_{c=1}^{k} \hat{n}_c^{|sp_{ic}|}}{k}, \; \overline{\hat{n}^{sd}} = \frac{\sum_{c=1}^{k} \hat{n}_c^{sd_{ic}}}{k}, \; \overline{\hat{n}^{sp}}, \overline{\hat{n}^{sd}} \in [0, 1] \quad (9)$$

$d_{N_i \to l}^{D(S^{(c)})}$ denotes the deviation between the moving state of N_i and those of all the items in $S^{(c)}$, according to eq. (10). The lower the value of $d_{N_i \to l}^{D(S^{(c)})}$ is, the lower the mobility difference between N_i and the items in $S^{(c)}$.

$$d_{N_i \to l}^{D(S^{(c)})} = \frac{|b_l \overline{\hat{n}^{sp}} - \overline{\hat{n}^{sd}} + c|}{\sqrt{1 + b_l^2}}, \quad d_{N_i \to l}^{D(S^{(c)})} \in [0, 1] \quad (10)$$

In eq. (10) b_l is the slope of the fitting line of $D(S^{(c)})$'s linear regression, according to eq. (11).

$$b_l = \frac{\sum\limits_{c=1}^{k} \hat{n}_c^{|sp_{ic}|}\hat{n}_c^{sd_{ic}} - k\widehat{\overline{n^{sp}}}\widehat{\overline{n^{sd}}}}{\sum\limits_{c=1}^{k} (\hat{n}_c^{sd_{ic}})^2 - k(\widehat{\overline{n^{sd}}})^2}, \quad b_l \in [-\infty, +\infty] \quad (11)$$

Eq. (12) introduces the information entropy generated by $S^{(p)}$.

$$I(S^{(p)}) = \begin{cases} -P^{(p)}\log_2 P^{(p)} & 0 < P^{(p)} < 1 \\ 0 & P^{(p)} = 0 \\ 1 & P^{(p)} = 1 \end{cases} \quad (12)$$

$$P^{(p)} = r^{D(S^{(p)})} \times (1 - d_{N_i \to l}^{D(S^{(p)})}), \; P^{(p)} \in [0, 1]$$

where the computational method of $P^{(p)}$ is the same with that of $P^{(c)}$ and was already described. The larger the value of $G(N_i)$ is, the lower the volatility is, which means the IN nodes of N_i tend to be relatively stable.

B. Self-regulated Period-based IN List Update Mechanism

As already mentioned, there is a need for a mechanism to manage the IN list updates for each node. A timer-based update scheme is employed which enables each mobile node update its one-hop neighbor list every T time units (e.g., T of the order of minutes, up to 1 hour) [33]. The algorithm involves two update period types: static and variable. The static update requires the mobile terminal to send periodically detection messages to all its one-hop neighbors. The update period setting directly influences both the accuracy and the cost of maintaining the IN list. For instance, a long update period reduces the number of detection messages and therefore the overhead, but some of the IN nodes might have changed their position and the list does not contain most up-to-date information. Conversely, a short update period ensures the information on the IN nodes is received in real-time; however this needs frequent exchange of detection messages and results in overhead increase.

In terms of considering a variable update period for each node N_i to manage its IN list in INR, this paper proposes a **Self-regulated Period-based Immediate-neighbor List Update Mechanism (SPUM)**. SPUM adaptively adjusts the update period in terms of IN nodes' volatility estimation. In this manner SPUM not only reduces the number of messages exchanged with the IN nodes, but also fast discovers CN candidates. For instance, whenever there are severe state variation of stable IN nodes in S, N_i should reduce its IN list update period to obtain higher amount of data, especially about the CN candidates. This enables faster estimation of stability variation in the process of stable CN discovery. Conversely, where the membership of IN nodes in S is stable, N_i should increase the update period to reduce the message overhead. Let ut_i be the variable information update period of N_i, with an initial value sv greater than 0. The update mechanism of ut_i is defined in eq. (13).

$$ut_i = ut_i^{(P)}(1 + R_i \times \sin(G(N_i))) \quad (13)$$

In eq. (13) ut_i and $ut_i^{(P)}$ are the current and previous values for the update period at node N_i, respectively and $G(N_i)$ is the variation level of moving state of IN nodes in S, as described in eq. (1). R_i is a weighted value to influence $G(N_i)$, according to eq. (14).

$$R_i = \frac{|S|}{|NL_i^{(new)}|}, R_i \in [0, 1] \quad (14)$$

In eq. (14) $|S|$ and $|NL_i^{(new)}|$ represent the number of items in S and $NL_i^{(new)}$, respectively. R_i is in fact the proportion of sample size ($|S|$) when calculating $G(N_i)$ relative to $NL_i^{(new)}$. The larger the value of R_i, the larger the level of regulating $ut_i^{(P)}$ is.

C. Membership Stability Estimation Model

As we know, the longer IN nodes remain in INR, the higher their membership stability is. We use a weighted solution to additively consider membership time in order to estimate the stability of each IN node. The variation levels of the movement speed and direction and spatial distance for each IN node $n_j \in S$ before and after updating INR are used as weight factors to calculate the membership stability of n_j.

(1)*weight factor for movement speed and spatial distance from N_i*. By making use of the Euclidean distance formula, the weight factor of n_j's speed and distance from N_i is obtained according to eq. (15).

$$vr_{ij} = \sqrt{(\hat{n}_j^{|sp_{ij}|} - (\hat{n}_j^{|sp_{ij}|})')^2 + (\hat{n}_j^{sd_{ij}} - (\hat{n}_j^{sd_{ij}})')^2} \quad (15)$$

where $\hat{n}_j^{|sp_{ij}|}$ and $(\hat{n}_j^{|sp_{ij}|})'$ are normalized values of n_j's average speed relative to N_i before and after updating INR, respectively. $\hat{n}_j^{sd_{ij}}$ and $(\hat{n}_j^{sd_{ij}})'$ are normalized values of n_j's distance from N_i before and after updating INR, respectively. The lower the value of $vr_{ij} \in [0, \sqrt{2}]$ is, the more stable the movement state of n_j is.

(2) **weight factor for movement direction**. $(X_j^{(C)}, Y_j^{(C)})$ and $(X_j^{(P)}, Y_j^{(P)})$ are current and previous geographic position coordinates of n_j for an update period at N_i, respectively. $(X_i^{(C)}, Y_i^{(C)})$ and $(X_i^{(P)}, Y_i^{(P)})$ are current and previous geographic position coordinates of N_i during the same update period, respectively. The movement traces of n_j and N_i generate two vectors $\vec{n}_j$ and $\vec{N}_i$ respectively according to eq. (16).

$$\begin{aligned} \vec{n}_j &= (X_j^{(C)} - X_j^{(P)}, Y_j^{(C)} - Y_j^{(P)}), \\ \vec{N}_i &= (X_i^{(C)} - X_i^{(P)}, Y_i^{(C)} - Y_i^{(P)}) \end{aligned} \quad (16)$$

We use the vector angle cosine of $\vec{n}_j$ and $\vec{N}_i$ to indicate the direction difference level in the movement trace between n_j and N_i according to eq. (17).

$$DR_{ij} = \cos\theta = \frac{\vec{N}_i \cdot \vec{n}_j}{|\vec{N}_i||\vec{n}_j|}, \cos\theta \in [-1, 1] \quad (17)$$

If $DR_{ij} \in (0,1]$, the movement direction of n_j is similar or consistent with that of N_i. If $DR_{ij} \in [-1,0)$, n_j and N_i have the inverse movement direction. If $DR_{ij} = 0$, the movement direction of n_j and N_i is orthogonal. The membership stability of the IN node n_j of N_i is obtained according to eq. (18).

$$st_{ij} = \begin{cases} st_{ij}^{(P)} + ut_i \times \cos(vr_{ij}) \times DR_{ij} & PD_{INR} > 0 \\ 0 & PD_{INR} = 0 \end{cases}$$ (18)

where st_{ij} and $st_{ij}^{(P)}$ ($st_{ij}, st_{ij}^{(P)} \in (-\infty, \infty)$) are the membership stability of n_j an IN node of N_i in current and previous update round, respectively. PD_{INR} is the number of update periods the IN node went through. $PD_{INR} = 0$ indicates that the IN node is a new entrant in INR. If $PD_{INR} > 0$, n_j is a stable IN node of N_i. $st_{ij} < 0$ and $st_{ij} > 0$ indicate that the movement trace of n_j and N_i is in the opposite and same direction in most update periods, respectively. The larger the stability value of IN nodes is, the higher the probability of IN nodes staying in INR is. Following these conclusions, the information associated with each item in NL_i is extended from a 2-tuple to a 3-tuple, as follows: $n_c \Leftrightarrow ((X_c, Y_c), sp_c, st_c)$ where st_c is the stability value.

D. Communication quality forecast model

As already mentioned, the path of cooperative fetching from supplier to N_i includes two parts: N_i to CN and CN to supplier. Before N_i fetches a new video sequence from the supplier n_x at t_{k+1}, it needs to investigate the communication quality in $path_{INs \to n_x}$ from IN nodes (CN candidates) to n_x and $path_{N_i \to INs}$ from N_i to IN nodes, in order to reduce the video resource fetching cost and download time.

(1) *estimation of communication quality in* $path_{INs \to n_x}$. N_i requires all members (their stability values are greater than 0) in the IN node subset $INS_i \Leftrightarrow (n_a, n_b, ..., n_h)$ to detect the available bandwidth to n_x. The available bandwidth set $AB_{jx}^{(O)} \Leftrightarrow (B_{jx}^{(O)}(t_1), B_{jx}^{(O)}(t_2), ..., B_{jx}^{(O)}(t_k))$ from each IN node n_j to n_x can be obtained as described in our previous work [36], where $t_1, t_2, ..., t_k$ denote the detection period time. The original series $AB_{jx}^{(O)}$ needs to be preprocessed to an accumulated series $AB_{jx}^{(A)} \Leftrightarrow (B_{jx}^{(A)}(t_1), B_{jx}^{(A)}(t_2), ..., B_{jx}^{(A)}(t_k))$, according to eq. (19):

$$B_{jx}^{(A)}(t_v) = \{\sum_{c=1}^{v} B_{jx}^{(O)}(t_c) | v = 1, 2, ..., k\}$$ (19)

By making use of the accumulated series $AB_{jx}^{(A)}$ to build the Grey Forecast Model $GM(AB_{jx}^{(A)})$ [34][35], the first-order differential equation of $GM(AB_{jx}^{(A)})$ is defined as in eq. (20):

$$\frac{dB^{(1)}}{dt} + aB^{(1)} = u$$ (20)

In eq. (20) t is the time series variable and B is the series variable of bandwidth accumulation with increasing detection time. a and u denote the Grey level of development and control, respectively. Eq. (21) describes the calculation method for solving the value of a and u according to the ordinary least square method.

$$\hat{U} = \begin{bmatrix} \hat{a} \\ \hat{u} \end{bmatrix} = (D^T D)^{-1} D^T y$$ (21)

In eq. (21) $\hat{a}$ and $\hat{u}$ solutions for a and u, respectively. D^T is the transposition matrix of D, $D = \begin{bmatrix} -\frac{1}{2}[B_{jx}^{(A)}(t_2) + B_{jx}^{(A)}(t_1)]1 \\ -\frac{1}{2}[B_{jx}^{(A)}(t_3) + B_{jx}^{(A)}(t_2)]1 \\ ... \\ -\frac{1}{2}[B_{jx}^{(A)}(t_k) + B_{jx}^{(A)}(t_{k-1})]1 \end{bmatrix}$ and $y = (B_{jx}^{(O)}(t_2), B_{jx}^{(O)}(t_3), ..., B_{jx}^{(O)}(t_k))^T$. Making use of $\hat{a}$ and $\hat{u}$ to solve eq. (20) we obtain eq. (22).

$$\hat{B}(v+1) = (B_{jx}^{(O)}(t_1) - \frac{\hat{u}}{\hat{a}})e^{-\hat{a}v} + \frac{\hat{u}}{\hat{a}}$$ (22)

$\hat{B}(v+1), v \leq k$ and $\hat{B}(v+1), v > k$ denote the fitting and forecast values, respectively. Let $C_{jx}(v) = B_{jx}^{(O)}(t_v) - \hat{B}_{jx}(v), v = 2, 3, ..., k$ denote the residual value. The residual mean value and variance is obtained according to eq. (23).

$$\bar{C}_{jx} = \frac{\sum_{c=2}^{k} C_{jx}(c)}{k-1}, F_{jx} = \sqrt{\frac{\sum_{c=1}^{k}(C_{jx}(c) - \bar{C}_{jx})^2}{k-1}}$$ (23)

The posteriori variance ratio $R_{jx}^{(P)}$ and its probability $P_{jx}^{(P)}$ are obtained according to eq. (24).

$$R_{jx}^{(P)} = \frac{F_{jx}}{\sigma_{jx}}, P_{jx}^{(P)} = P\{|C_{jx}(v) - \bar{C}_{jx}| < 0.6745\sigma_{jx}\}$$ (24)

where σ_{jx} is the variance of bandwidth in k update periods. σ_{jx} is defined as in eq. (25).

$$\sigma_{jx} = \sqrt{\frac{\sum_{c=1}^{k}(B_{jx}^{(O)}(t_c) - \bar{B}_{jx}^{(O)})^2}{k}}, \bar{B}_{jx} = \frac{\sum_{c=1}^{k} B_{jx}^{(O)}(t_c)}{k}$$ (25)

$R_{jx}^{(P)}$ and $P_{jx}^{(P)}$ can reflect the volatility level of bandwidth in the path of data delivery during the detection period time, so they are used to estimate the link reliability in the path of data transmission. We set two threshold values $TH^{(R)}$ and $TH^{(P)}$ in the context of the Grey Forecast Model in order to measure the link reliability in the transmission path. If $R_{jx}^{(P)} \geq TH^{(R)}$ and $P_{jx}^{(P)} \geq TH^{(P)}$, the link state of $path_{jx}$ is reliable. N_i filters out all the members which have unreliable links in INS_i and obtains a new IN subset INX_i.

(2) **The estimation approach of communication quality in** $path_{N_i \to INs}$ is the same with that of $path_{INs \to n_x}$. N_i detects the available bandwidth to each member n_h in INS_i and obtains a bandwidth set $AB_{ih}^{(O)}$ and an accumulated series $AB_{ih}^{(A)}$ according to eq. (19). In terms of solution of the built Grey Forecast Model $GM(AB_{ih}^{(A)})$, we can obtain the posteriori variance ratio $R_{ih}^{(P)}$ and $P_{ih}^{(P)}$. We still use $TH^{(R)}$ and $TH^{(P)}$ to evaluate the reliability of link state of $path_{ih}$. N_i filters out the unreliable members in INS_i and also obtains a new IN subset INI_i.

The members of $INX_i \cap INI_i$ are considered CN candidates. We need to calculate the bandwidth forecast expectation value $\bar{B}_{ix}^{(F)} = min(\bar{B}_{ij}^{(F)}, \bar{B}_{jx}^{(F)})$ for each member n_j in $INX_i \cap INI_i$ at $[t_{k+1}, t_v], v \in [k+1, 2k]$. This is done according to eq. (22).

E. Cooperative Fetching Algorithm

In order to select the appropriate CN, we make use of the Grey Relational Analysis (GRA) [37] to estimate the forecast bandwidth and stability of these CN candidates. The stability and forecast bandwidth are considered as the estimated parameters and are normalized according to eq. (26).

$$x_{ij}^*(att) = \frac{x_{ij}(att) - lower_{att}}{upper_{att} - lower_{att}}, \; x_{ij}^*(att) \in [0,1] \quad (26)$$

In eq. (26) att and $x_{ij}(att)$ denote estimated parameter (stability and forecast bandwidth) of n_j and its value, respectively. $lower_{att}$ and $upper_{att}$ are minimum and maximum corresponding to the current estimated parameter att for all CN candidates, respectively. The Grey Relational Coefficient (GRC) of these candidates is obtained according to eq. (27).

$$GRC_{ij} = \frac{1}{\sum w_{att}|\dot{x}_{ij}^*(att) - 1| + 1}, \; GRC_{ij} \in [0,1] \quad (27)$$

In eq. (27), w_{att} is the weight value of $x_{ij}^*(att)$ and each parameter has a different value of w_{att}. If we focus on the stability, the value of w_{att} associated to stability should be greater than that of bandwidth. The candidate which has the maximum value of GRC is selected as N_i's CN. Consequently N_i sends a cooperative fetching request message to CN and makes preparations for receiving streaming data from the CN. The request message between nodes has the following format: $req = (vID, spt, len, source)$, where vID identifies the requested video sequence, spt and len are the start point and length of the required video chunk, respectively and $source$ is the source supplier which has the video content. As soon as the CN receives the video data from n_x, it forwards the received data to N_i. The pseudo-code of the above process is detailed in Algorithm 1.

F. Computation Complexity

We analyze the computation complexity of CCF in the process of CN selection. (1) CCF estimates the mobility stability of the items in S which have experienced one or multiple update period(s) of N_i and are considered as CN candidates. The computation complexity for calculating the volatility and stability of mobility of IN nodes is $O(v)$ during an update period of IN nodes, where v is the length of S. The number of the items in S determines the cost for the calculation of mobility stability of IN nodes. With increasing update times of IN nodes, the computation complexity is $O(rv)$, where r denotes the number of times of updating the IN nodes. (2) CCF selects the IN nodes whose stability values are greater than 0 from S to detect and estimate the communication quality in the path of cooperative fetching. The

---

Algorithm 1 Cooperative fetching algorithm for N_i
1: $//count(S)$ is the size of S set;
2: **for**$(j = 0; j < count(S); j++)$
3:      computes stability st_{ij} for each IN $S[j]$ by eq. (18);
4:      **if** $st_{ij} > 0$
5:          put $S[j]$ into INS_i
6:      **end if**
7: **end for** j
8: **for**$(j = 0; j < count(INS_i); j++)$
9:      computes posteriori variance ratio $R_{jx}^{(P)}, P_{jx}^{(P)}, R_{ij}^{(P)},$ $P_{ij}^{(P)}$ for each IN node $INS_i[j]$ by eq. (24);
10:     **if** $R_{jx}^{(P)} \geq TH^{(R)}$ && $P_{jx}^{(P)} \geq TH^{(P)}$
11:         put $INS_i[j]$ into INX_i;
12:     **end if**
13:     **if** $R_{ij}^{(P)} \geq TH^{(R)}$ && $P_{ij}^{(P)} \geq TH^{(P)}$
14:         put $INS_i[j]$ into INI_i;
15:     **end if**
16: **end for** j
17: **for**$(j = 0; j < count(CNS_i = INX_i \cap INI_i); j++)$
18:     normalizes evaluation attribution of $CNS_i[j]$ by eq. (26);
19:     calculates GRC of $CNS_i[j]$ by eq. (27);
20: **end for** j
21: selects item n_j which has maximum value of GRC in CNS_i;
22: send request message to n_j;
23: N_i makes preparations for receiving forwarded data from n_j;
24: N_i receives multimedia data;

---

selected IN nodes form a subset $INS_i \in S$. The computation complexity of communication quality is $O(v)$. (3) The items in INS_i which have the reliable link in the path of cooperative fetching form the CN candidate set CNS_i. CCF selects the CN from CNS_i in terms of their predicted bandwidth and stability. The computation complexity of CN selection algorithm is $O(v)$ due to $CNS_i \in S$. The computation complexity of CCF is $O(rv)$.

IV. PERFORMANCE EVALUATION

A. Simulation Settings and Scenarios

The transmission efficiency of video data in the path of cooperative fetching determines the performance of this fetching. CCF divides the path into two parts: from the downloader to CN and from CN to the content supplier, and employs two models to address the problems in the delivery capacity of video content caused by the mobility of mobile nodes. (1) CCF investigates the mobility stability of the IN nodes to ensure a stable one-hop neighbor relationship between the downloader and CN, which obtains high transmission capacity in the path from the downloader to CN. (2) CCF estimates the link reliability and forecasts the bandwidth in the path of cooperative fetching. The performance of the proposed CCF is compared against two classic algorithms: the Geographical Distance-based Neighbor selection (GDN) and Available Bandwidth-based Neighbor selection (ABN), which are described in [22]. GDN focuses on the geographical distance between the downloader and CN, so the CN node selected needs to have the closest geographical distance to the downloader. ABN investigates the communication quality in the path from CN to content supplier, so the one-hop neighbor which has the highest bandwidth to the content supplier is considered as a CN node. Therefore, GDN and ABN are similar to CCF in the CN selection strategy and are suitable

for the performance comparison with CCF. Network Simulator version 2 (NS-2) is used for modeling and simulations. Next the setup for the common simulation environment for testing the three solutions is discussed. Table II lists some important NS2 simulation parameters of the wireless network.

In order to perform a closer-to-reality simulation in a mobile wireless network environment, we defined six simulation scenarios in which the mobile speed of nodes is set to the following six ranges: [1-5], (5-10], (10-15], (15-20], (20-25] and (25-30] m/s. When a mobile node reaches the specified destination, it immediately restarts its movement with a new assigned speed and destination. As ABN and GDN do not update the IN list, we assume they use a static timer-based update scheme in order to compare the maintenance overhead of IN nodes with ABN and GDN. Previous research studied the effect of setting of the static update period [33]. Short periods (1-2 seconds) obtain fast real-time information about the IN nodes, but incur high message overhead. On the contrary, long periods (7-10 seconds) reduce the message overhead, but cannot obtain the state of the one-hop neighbors in real-time. In order to balance the maintenance cost and fast obtain the real-time state of one-hop neighbors, the update period time of ABN and GDN is set to 4.5 s. The initial update period time sv in CCF is set to 1 s. The two thresholds $T^{(R)}$ and $T^{(P)}$ in terms of the evaluation model in Grey Forecast Model [34][35] are set to 0.5 and 0.8, respectively. The weight factors of stability and bandwidth in eq. (27) are set to 0.5. ABN, GDN and CCF select 10 mobile nodes as the requesters. The period time of detection bandwidth is set to 10 s. After estimation and forecast of communication quality, these requesters select their CN nodes and require them to fetch the video chunk from the server. The length of video chunk is set to 30 s. When these

TABLE II
SIMULATION PARAMETER SETTINGS FOR THE WIRELESS NETWORK

Parameters	Values
Area	$800 \times 800 (m^2)$
Antenna Type	Antenna/OmniAntenna
Bandwidth of Each Mobile Node	2 Mb/s
Channel	Channel/WirelessChannel
Default Distance between Server and Nodes	6 hops
802.11 Data Transmission Rate	2 Mb/s
802.11 Basic Transmission Rate	1 Mb/s
Interface Queue Type	CMUPriQueue
Length of Video Chunk	30 s
MAC Interface	MAC/802_11
Movement Direction of Each Mobile Node	Random
Network Interface	Phy/WirelessPhy
n_{MAX}^{sd}	200 m
n_{MAX}^{sp}	100 m/s
Number of Mobile Nodes	400
Peak Mobility Speed	30 m/s
Pause time of Each Mobile Node	0 s
Rate of Streaming Data	480 kb/s
Routing Protocol	DSR
Simulation Time	410 s
Transmission Protocol of Video Data	UDP
Transmission Protocol of Control Messages	TCP
Wireless Signal Range	200 m

requesters have received 30 s streaming data, they re-select the CN node after the estimation and forecast of communication quality and receive the data from the CN nodes. The number of iterations is set to 10. The six simulation scenarios are repeatedly tested six times, respectively.

B. Performance Evaluation

The performance of CCF is compared with that of GDN and ABN in terms of average CN selection accuracy, average end-to-end delay, average packet loss ratio (PLR), average throughput, maintenance overhead of the IN nodes and estimated user perceived quality measured by Peak Signal-to-Noise Ratio (PSNR) as defined by eq. (14) [38]. These metrics are computed for different mobility levels of the nodes. Increasing mobility is considered in terms of the six speed intervals. This is as the mobile nodes' speed is a significant factor in the process of CN selection. The mean value of simulation results of six repeated testing for each simulation scenario is used to illustrate the performance difference between the three strategies compared.

(1) *Average CN selection accuracy*. The request nodes (requesters) select CN from their IN nodes to obtain the requested video chunk. The selected CNs connect with the media server and forward the video data from the server to the requesters. The above process of cooperative fetching also is considered as a CN selection problem. If the selected CN maintains the IN relationship with the requester in the process of cooperative fetching, the CN selection is considered accurate. The number of accurate selection times divided by the number of total CN selection times is used to indicate the average CN selection accuracy.

Fig. 4 shows the average CN selection accuracy with increasing node mobility. The blue curve shows how CCF CN selection accuracy has high values between 0.8 and 1, despite a slight decrease with the increase in node mobility. The red curve indicates how GDN's results drop sharply with increasing node mobility from initial high average CN selection accuracy to a value of 0.45, more than 70% lower than that of CCF. The green curve corresponding to ABN also decreases with increasing node mobility, but its corresponding accuracy values are always much lower than those of CCF and GDN.

The figure clearly shows how CCF outperforms GDN and ABN in terms of performance. By considering the stability value for the IN nodes, the requesting node and CN nodes have similar speed and direction and the IN relationship is maintained over a relative long-term period. Consequently, the increasing node mobility variation does not affect the performance of CCF. In GDN, the CN nodes stay close to the requesting node in the transitory period, but rapidly lose the IN relationship with the requester when the mobility increases. The selection strategy of CN node in ABN relies on bandwidth to server estimation, neglecting any location-related factors. Therefore, for ABN, the higher the node mobility is, the lower the average CN selection accuracy is.

(2) *Average end-to-end delay*. The requesters select CN from their IN nodes to obtain the requested video chunk with
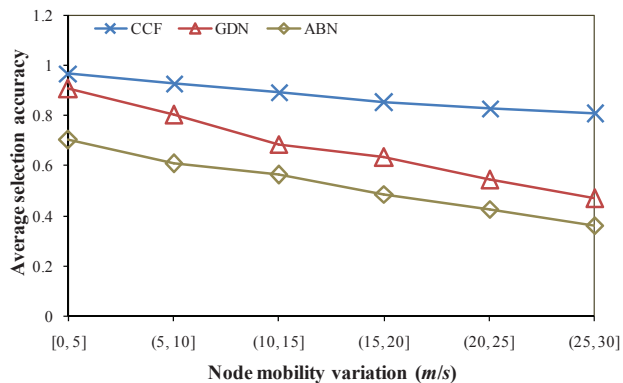
Fig. 4. Average CN selection accuracy

Fig. 5. Average end-to-end delay

a length of 30 s. The selected CNs connect with the media server to obtain the video chunk. The server transmits the video chunk at the 480 kb/s data transmission rate. The CNs use the same transmission rate to forward the received data to the requesters. The delay of video data received by CNs and requesters is used to indicate the end-to-end delay, namely the mean value of average transmission delay of two paths: from server to CNs and from CNs to requesters is considered as average end-to-end delay in the wireless network. The average delay is defined as:

$$\overline{AD} = \frac{\sum\limits_{i=1}^{m} D_i^{(r)} + \sum\limits_{j=1}^{n} D_j^{(c)}}{N(s) + N(c)} \tag{28}$$

where $\sum\limits_{i=1}^{m} D_i^{(r)}$ and $\sum\limits_{j=1}^{n} D_j^{(c)}$ are the delay of the data received by requesters and CN nodes, respectively. $N(s)$ and $N(c)$ are the data items received by requesters and CN nodes, respectively.

In Fig. 5, we illustrate how the average end-to-end delay varies with the increase in the node mobility variance, when CCF, ABN and GDN are used in turn. It can be seen how the average end-to-end delays of ABN and GDN are maintained at relatively high levels and increase fast (the delay values are between 0.08 s and 0.25 s). CCF's average end-to-end delay curve keeps a low level with slight increase during the mobile nodes' increase in mobility. The delay values are between 0.02 s and 0.07 s, three times than those of ABN and GDN. The results shown by Fig. 5 also indicate how with increasing node mobility, CCF's performance benefits become even more evident.

The up to 300% better CCF results than those of ABN and GDN are due to the fact that CCF monitors the IN nodes and estimates their stability. The stability measurement for IN nodes ensures the CNs maintain the IN relationship with the requester for longer. By estimating the stability of each IN, the influence of mobile nodes' mobility on CCF's performance is reduced, unlike ABN and GDN. Moreover, CCF makes use of the estimation and forecast of communication quality in the server-to-CN and CN-to-requester paths. The high available bandwidth and reliable link state ensure low average end-to-end delay. In GDN and ABN, the selected CN only depends on
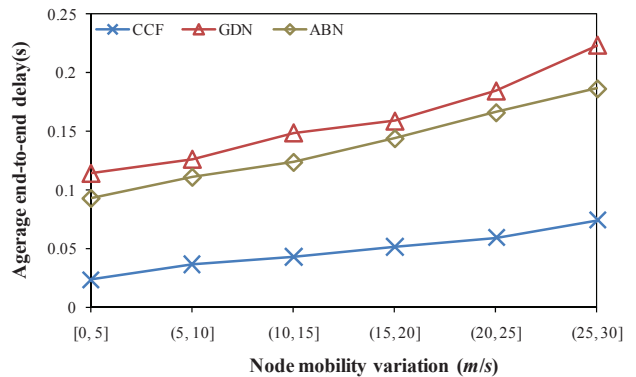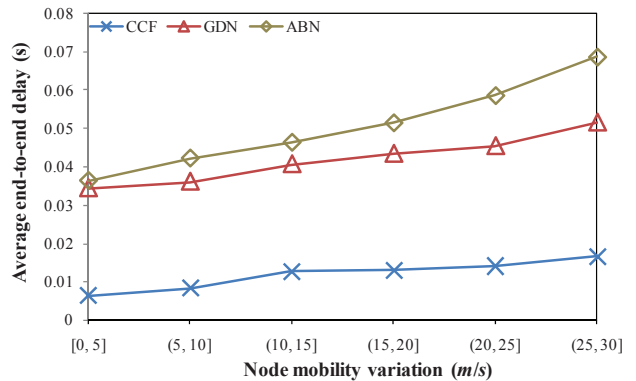

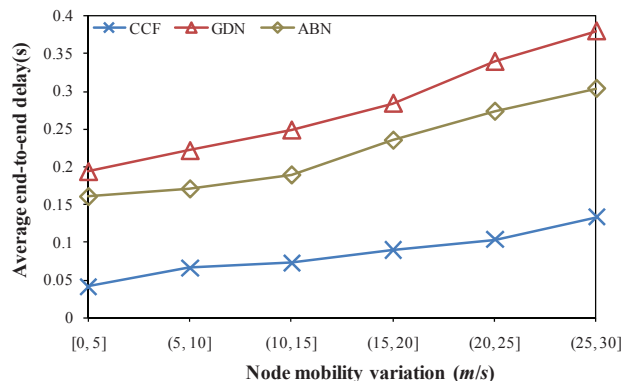Fig. 6. Average end-to-end delay in the CN-to-requester path

Fig. 7. Average end-to-end delay in the server-to-CN path

the instantaneous closest geographical distance to the requester and highest bandwidth value from CN node to server, but the closest distance and highest bandwidth are dynamically changing with the movement of mobile nodes. With increasing mobile nodes' speed, the rapidly increasing distance between two nodes and high dynamic network topology increasingly affect the performance of video data delivery.

In order to clarify further the average delay, we illustrate the average end-to-end delay in the CN-to-requester and server-to-CN paths in Fig. 6 and Fig.7.

Average end-to-end delay in the CN-to-requester path: The average end-to-end delay in the CN-to-requester path is

defined as:

$$\overline{AD_{c \to r}} = \frac{\sum\limits_{i=1}^{m} D_i^{(r)}}{N(s)} \qquad (29)$$

where $\overline{AD_{c \to r}}$ denotes the average delay in the CN-to-requester path. Fig. 6 shows the average delay in CN-to-requester path for CCF, ABN and GDN with increasing node mobility variance. The curves corresponding to the results of ABN and GDN are at the high levels and have rapidly increasing trends (i.e. GDN's curve increases from 0.03 s to 0.05 s and ABN's results have faster increase than GDN from 0.03 s to 0.07 s). The curve corresponding to the CCF results experiences a slow increase and slight fluctuations, with values roughly 300% lower than those of ABN and GDN. Fig. 6 clearly shows how CCF outperforms ABN and GDN in terms of performance.

CCF investigates the IN nodes' speed and direction of movement and geographical distance from the requester in order to estimate their stability. If CN nodes have stable IN relationship with the requester, the data delivery over one-hop is performed with low delay. Moreover, monitoring and forecasting of communication quality in the CN-to-requester path ensures high available bandwidth and reliable link state. The relatively good communication quality reduces the average delay between the requester and CN node. GDN selects CN nodes in terms of close geographical distance to requester and neglects the communication quality between CN nodes and requester. Increasing distance between CN node and requester with mobility variation of nodes results in higher average delay in the CN-to-requester path than for the case when CCF is employed. The selection of CN nodes in ABN relies on the bandwidth between CN nodes and the server and it does not consider the key factors - distance and bandwidth from the CN node to the requester. Consequently, in increasing node mobility conditions, ABN has the highest average delay among CCF, ABN and GDN.

Average end-to-end delay in the server-to-CN path: The average end-to-end delay in the server-to-CN path is defined as:

$$\overline{AD_{s \to c}} = \frac{\sum\limits_{i=1}^{n} D_i^{(c)}}{N(c)} \qquad (30)$$

where $\overline{AD_{s \to c}}$ denotes the average delay in the server-to-CN path. Fig. 7 shows the average end-to-end delay in the server-to-CN path for CCF, ABN and GDN, respectively. The average delays of ABN and GDN are maintained at high levels and grow fast from 0.15 s to 0.4 s with the increase in node mobility. It can be noted that the delay values and increase range of GDN are higher than those of ABN. CCF's delays are kept low and experience slight growth from 0.04 s to 0.13 s only with node mobility. As the CCF average delay values are roughly 200% lower than those of ABN and GDN, it can be concluded that CCF outperforms ABN and GDN in terms of delay-related performance.
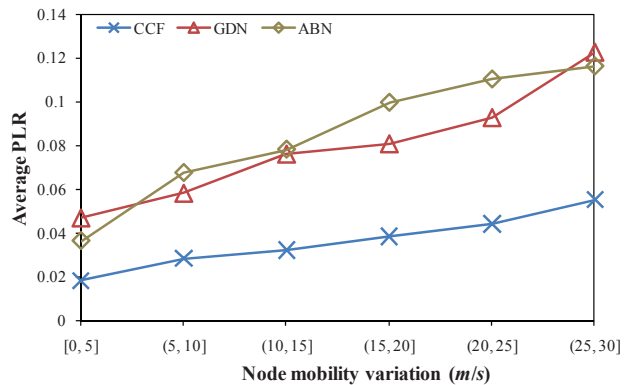

Fig. 8. Average Packet Loss Ratio

CCF not only investigates the link reliability of CN node in the server-to-CN path, but also forecasts the available bandwidth to the server. The relatively good communication quality between CN node and server enhances the efficiency of data delivery and reduces the delay. The CN nodes have the highest bandwidth to the server in ABN, but ABN does not evaluate the link reliability and does not forecast the available bandwidth, which can change fast in a dynamic network environment and negatively influence the efficiency of data transmission. Unlike CCF and ABN, CN nodes in GDN do not have any a priori "knowledge" of bandwidth in the server-to-CN path, so GDN's delay values are the highest among the three solutions studied.

(3) *Average packet loss ratio (PLR)*. The total number of lost packets divided by the total number of sent packets indicates the PLR. The mean value of PLR of two paths: from server to CNs and from CNs to requesters is considered as average PLR in the wireless network. Fig. 8 illustrates the variation of the average PLR for CCF, GDN and ABN with the increase in mobile nodes' mobility. In general, average PLR of GDN and ABN is maintained relatively high (between 0.04 and 0.13) and presents rapid growth with increasing mobile nodes' mobility. At the same time, CCF's average PLR has low values and exhibit slow increase, less than 0.05 during the whole duration of the tests. The results shown in Fig. 6 clearly indicate how CCF outperforms both GDN and ABN in terms of PLR-based performance.

As already known, high transmission efficiency and low PLR are direct effects from having good communication quality in the transmission path. By making use of monitoring and forecasting of communication quality in the server-to-CN and CN-to-requester paths, CCF selects CN nodes which have both high available bandwidth and reliable links to cooperatively fetch video content, so the average PLR is maintained low. ABN only considers the bandwidth from the CN node to the server, so it cannot cope with variation of communication quality in the server-to-CN and CN-to-requester paths with increasing mobility of mobile nodes. GDN does not consider the factors relative to communication quality so that it cannot ensure low PLR. On the other hand, the large number of intermediate nodes in the transmission path increases the probability of packet loss. CCF, by estimating the stability
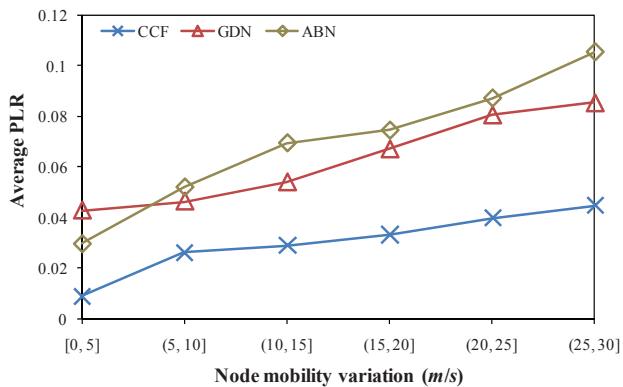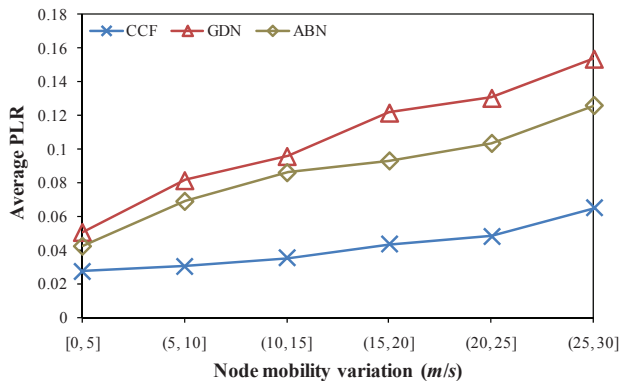
Fig. 9. Average PLR in CN-to-requester path

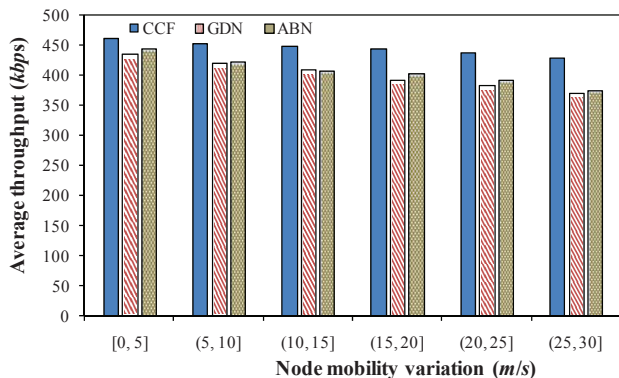Fig. 10. Average PLR in the server-to-CN path

Fig. 11. Average throughput

Fig. 12. Average PSNR

Average PLR in the CN-to-requester path: Fig. 9 plots the average PLR between the requester and CN nodes for CCF, ABN and GDN with increasing mobility of mobile nodes. PLR values for ABN and GDN present rapidly increasing trends, from 0.04 to 0.08 for GDN and from 0.03 to 0.13 for ABN. CCF's values shows low increases, with values roughly 200% lower than those of ABN and GDN.

By investigating the mobility-related factors of the IN nodes - speed, direction and geographical distance from the requester, CCF estimates the stability in terms of their movement. The long-term IN relationship between the requester and CN nodes ensures low PLR, namely the one-hop delivery can reduce the packet loss probability. Moreover, by making use of the monitoring and forecasting of communication quality, the reliable link state and high available bandwidth enhance the success rate of data delivery. Unlike CCF, GDN does not deal well with the mobility of mobile nodes. The CN which has the closest geographical distance with the requester may fast leave the INR of requester so that the multi-hop transmission between CN and requester increases PLR. Moreover, GDN does not consider the communication quality between the CN node and requester, so GDN's PLR presents fast increase. In ABN, the selection of CN node depends on the bandwidth between the CN node and server so that the distance and communication quality relative to the requester are neglected. In low node mobility situations, ABN has similar PLR with GDN, but its PLR fast rises with increasing mobility levels. Consequently, the performance of video data delivery increasingly declines due to the growing distance between the requester and CN selected.

Average PLR in the server-to-CN path: As Fig. 10 shows, the average PLR between the server and CN nodes of CCF, ABN and GDN maintains a rising trend with increasing mobility variation of mobile nodes. PLR of ABN and GDN fast increase from 0.04 to 0.13, and from 0.05 to 0.15, respectively. PLR values and increase range of GDN are higher than those of ABN. CCF's PLR values are maintained at low levels, roughly 2000% lower than those of ABN and GDN, and have a slow rise from 0.02 to 0.06.

By monitoring and forecasting the communication quality from the IN nodes to server, CCF can discover the CN nodes which have relatively good communication quality in the

of each IN node, maintains stable the IN relationship between CN and requester relatively long-term with increasing mobile nodes' mobility, so CCF's average PLR in the CN-to-requester path is kept very low. GDN relies on close distance between the CN and requester which changes fast with increasing node mobility, so GDN's average PLR in the requester-to-CN path rises relatively fast. ABN neglects the location factor relative to the requester so the increasing distance between the CN node and requester leads to PLR increase in the requester-to-CN path with the increase in the mobility of mobile nodes.

Fig. 9 and Fig. 10 illustrate the average PLR in the CN-to-requester and server-to-CN paths.
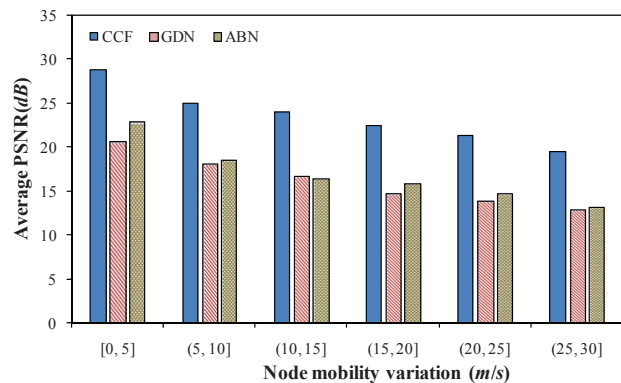
server-to-CN path. CCF's PLR is kept low with increasing mobility of the mobile nodes. In ABN, the CN node has the highest bandwidth value in the server-to-CN path. The bandwidth value in the dynamic network environment may have severe fluctuations, so ABN's PLR values fast rise with the mobility variation of mobile nodes. GDN is unaware of bandwidth and link state in the server-to-CN path, so GDN's PLR values vary the most in comparison with CCF and ABN.

(4 and 5) *Average throughput and video quality*. The average throughput is defined as:

$$\overline{THR} = \frac{\sum\limits_{i=1}^{m} SZ_i^{(r)}}{m * h * time^{(r)}} \quad (31)$$

where $\sum\limits_{i=1}^{m} SZ_i^{(r)}$ is the amount of data received by all requesters. m and h are the number of requesters and cooperative fetching, respectively. $time^{(r)}$ is the time sum of receiving data. $\overline{THR}$ denotes the average throughput obtained by every requester in a cooperative fetching process.

Fig. 11 compares the average throughput of CCF, ABN and GDN. The blue histograms corresponding to CCF results outperform ABN and GDN (red and green histograms), with roughly 10%. ABN and GDN have similar results in terms of performance difference relative to CCF with increasing mobility variation of mobile nodes.

Video quality, expressed in PSNR and measured in decibels (dB), is estimated according to eq. (32) as video quality gets influenced by the delivery through the communication channel [38].

$$PSNR = 20 \cdot \log_{10}(\frac{MAX\_Bitrate}{\sqrt{(EXP\_Thr - CRT\_Thr)^2}}) \quad (32)$$

In eq. (30) $MAX\_Bitrate$ is the average bitrate of the multimedia stream as resulted from the encoding process, EXP_Thr denotes the average throughput expected from the delivery of the multimedia stream over the network and CRT_Thr indicates the actual throughput measured during delivery. $MAX\_Bitrate$ and EXP_Thr are 480 kb/s in terms of simulation settings, respectively. We make use of $\overline{THR}$ to obtain PSNR of single video streaming corresponding to every requester in a cooperative fetching process.

Fig. 12 shows the average video quality corresponding to the average throughput of CCF, ABN and GDN with increasing mobility of the mobile nodes. The blue bars correspond to CCF's results and have initial high average values, close to 30 dB, excellent in terms of video quality. Despite high node mobility increase, the CCF video quality decreases down to a minimum of 20 dB, which is still considered good for wireless transmissions more than 50% higher than those of ABN and GDN. The red histograms corresponding to ABN's results are similar with those of GDN and drop from good video quality levels of roughly 20 dB in low node mobility situations to low quality levels of 15 dB with increasing mobility variation.

CCF makes use of monitoring and forecasting of stability and communication quality to obtain the high delivery performance of video data. CCF's maintains average throughput at high levels, which in conjunction with low PLR, results in high quality levels for video streaming. However, ABN and GDN do not adapt well to the dynamic network environment so that they have both lower throughput and higher PLR and consequently, lower quality levels for video data delivery.

(6) *Maintenance overhead of the IN nodes*. The maintenance overhead is expressed in terms of number of messages required for the IN nodes selection for every requester. The maintenance overhead relies on the number of IN nodes and update period time. The more IN nodes and less update period can increase the maintenance cost. The purpose of comparison for GDN, ABN and CCF in maintenance overhead shows the performance difference between static and dynamic update period.

Fig. 13 (a), (b) and (c) show how the maintenance overhead of the IN nodes varies withthe increasing mobility of the mobile nodes when the number of mobile nodes increases from 400 to 500 and 600, respectively. The value of every bar denotes the number of messages exchanged between the requester and the IN nodes in given speed range of node mobility.

The red and green histograms correspond to the results of GDN and ABN, respectively. GDN and ABN employ a static timer-based update scheme for maintaining IN nodes, so they have the same maintenance overhead. GDN and ABN have both higher values and fast decrease trends with the increase in the speed variation of mobile nodes in the different number of mobile nodes. Their maintenance overhead are in [4000, 15000], [5000, 18000] and [6000, 20000] ranges corresponding to 400, 500 and 600 mobile nodes, respectively. The maintenance overhead of GDN and ABN rises with increasing number of mobile nodes. The CCF results, illustrated with blue bars are in [1500, 2500], [1600, 2600], [1800, 2800] ranges with increasing number of mobile nodes, with lower values and variations than those of GDN and ABN. The maintenance overhead in CCF presents arising trend with the increasing mobility of mobile nodes, too, but the increment is much lower. This determines the results of GDN and ABN to be between 800% and 200% higher than those of CCF, respectively, CCF outperforming both GDN and ABN.

The main reason for this difference between the three solutions is that the requester in CCF regulates the update period time in terms of the variation level of the IN nodes: the mobile nodes increase the update period to reduce the update frequency when the number of stable IN nodes is high and decrease the update period to increase the update frequency otherwise. CCF also has low maintenance overhead in different node density situations, so the variations in number and mobility of mobile nodes influences CCF slightly only. The continuous self-regulation characteristic of CCF (which perceives the variation of IN nodes membership stability) makes sure the performance advantage is in favor of CCF. In GDN and ABN, the performance is limited due to the static update period. As the movement speed variation of nodes is low (e.g., node speeds are between [1-5] or (5-10]), the IN nodes maintain relative stable INRs as mobile nodes with low speed need several update periods before they leave their INRs. In this situation the number of detection
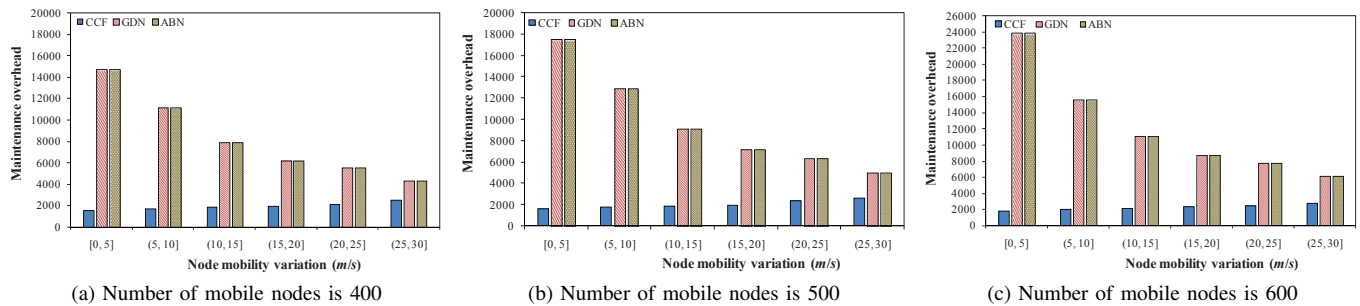
Fig. 13. Maintenance overhead

messages is maintained high (between many nodes), which is unnecessary. As the movement speed of nodes increases, the number of detection messages decreases. This is as many nodes leave INR and few stable IN nodes are left with which data is exchanged until new nodes are joining. These new nodes would have to wait until the next static update period to exchange data, which is sub-optimal. GDN and ABN have the lower adaptability for dynamic network environment than CCF. Consequently CCF outperforms GDN and ABN also in terms of maintenance overhead.

V. CONCLUSION AND FUTURE WORK

This paper proposes *CCF, a novel Cooperative Content Fetching-based strategy to increase the quality of video delivery to mobile users in wireless networks*. By monitoring the movement of the one-hop neighbors and employing an innovative forecast model for communication quality which measures the link reliability and predicts the bandwidth in the transmission path, CCF estimates cooperative neighbor (CN) characteristics in terms of both stability and communication quality. CCF considers the CN node selected as extensions of the local buffer and proposes an efficient cooperative fetching algorithm to improve video quality levels. CCF's performance was assessed in comparison with that of two classic CN selection strategies - GDN and ABN via simulations. The results show how CCF outperforms both GDN and ABN in terms of CN selection accuracy, average end-to-end delay, average packet loss ratio, maintenance overhead, average throughput and video quality levels in increasing node mobility conditions.

Future work will integrate existing concurrent multipath transfer mechanism (e.g. SCTP and MPTCP) [39]-[41] to propose CN-cooperated multipath transfer solution in order to enhance further the performance of video data transmission.

REFERENCES

[1] R. Trestian, O. Ormond and G.-M. Muntean, "Enhanced Power-Friendly Access Network Selection Strategy for Multimedia Delivery Over Heterogeneous Wireless Networks," *IEEE Trans. on Broadcasting*, vol. 60, no. 1, pp. 85-101, Mar. 2014.

[2] Z. Shen, J. Luo, R. Zimmermann and A.V. Vasilakos, "Peer-to-Peer Media Streaming Insights and New Developments," *Proceedings of the IEEE*, vol. 99, no. 12, pp. 2089-2109, Dec. 2011.

[3] L. Zhou, X. Wang, W. Tu, G.-M. Muntean and B. Geller, "Distributed Scheduling Scheme for Video Streaming over Multi-Channel Multi-Radio Multi-Hop Wireless Networks," *IEEE Journal on Selected Areas in Communications*, vol. 28, no. 3, pp. 409-419, Apr. 2010.

[4] L. Zhou, R. Hu, Y. Qian and H.-H. Chen, "Energy-Spectrum Efficiency Tradeoff for Video Streaming over Mobile Ad Hoc Networks," *IEEE Journal on Selected Areas in Communications*, vol. 31, no. 5, pp. 981-991, May 2013.

[5] C. Xu, G.-M. Muntean, E. Fallon and A. Hanley, "Distributed storage-assisted data-driven overlay network for P2P VoD services," *IEEE Trans. on Broadcasting*, vol. 55, no. 1, pp. 1-10, Mar. 2009.

[6] W. Yao, L.-P. Chau and S. Rahardja, "Joint Rate Allocation of Stereoscopic 3D Videos in Next-Generation Broadcast Applications," *IEEE Trans. on Broadcasting*, vol. 59, no. 3, pp. 445-454, Sept. 2013.

[7] K. Wang, M. Barkowsky, K. Brunnstrom, M. Sjostrom, R. Cousseau and P. Le Callet, "Perceived 3D TV Transmission Quality Assessment: Multi-Laboratory Results Using Absolute Category Rating on Quality of Experience Scale," *IEEE Trans. on Broadcasting*, vol. 58, no. 4, pp. 544-557, Dec. 2012.

[8] N. Narita and M. Kanazawa, "Analysis of Psychological Factors for HDTV/3-D HDTV and Evaluation Method of Their Overall Impressions," *IEEE Trans. on Broadcasting*, vol. 59, no. 1, pp. 13-19, Mar. 2013.

[9] Y. Chang and K. Munchurl, "A Joint Rate Control Scheme in a Hybrid Stereoscopic Video Codec System for 3DTV Broadcasting," *IEEE Trans. on Broadcasting*, vol. 59, no. 2, pp. 265-280, June 2013.

[10] S. Jia, C. Xu, A. V. Vasilakos, J. Guan, H. Zhang and G.-M. Muntean, "Reliability-oriented Ant Colony Optimization-based Mobile Peer-to-peer VoD Solution in MANETs," *ACM/Springer Wireless Networks*, In Press, Nov. 2013.

[11] C. Xu, S. Jia, L. Zhong, H. Zhang and G.-M. Muntean, "Ant-Inspired Mini-Community-Based Solution for Video-On-Demand Services in Wireless Mobile Networks," *IEEE Trans. on Broadcasting*, vol. pp, no. 99, Apr. 2014.

[12] S. Jia, C. Xu, G.-M. Muntean, J. Guan and H. Zhang, "Cross-Layer and One-Hop Neighbour-Assisted Video Sharing Solution in Mobile Ad Hoc Networks," *China Communications*, vol. 10, no. 6, pp. 111-126, June 2013.

[13] S.-B. Lee, A. F. Smeaton and G.-M. Muntean, "Quality-Oriented Multiple-Source Multimedia Delivery Over Heterogeneous Wireless Networks," *IEEE Trans. on Broadcasting*, vol. 57, no. 2, pp. 216-230, June 2011.

[14] L. Tu and C.-M. Huang, "Collaborative Content Fetching Using MAC Layer Multicast in Wireless Mobile Networks," *IEEE Trans. on Broadcasting*, vol. 57, no. 3, pp. 695-706, Sept. 2011.

[15] B. Chen and M. Chan, "MobTorrent: A Framework for Mobile Internet Access from Vehicles," *Proc. IEEE International Conference on Computer Communications (INFOCOM)*, Apr. 2009.

[16] H. Shirazi, J. Cosmas and D. Cutts, "A Cooperative Cellular and Broadcast Conditional Access System for Pay-TV Systems," *IEEE Trans. on Broadcasting*, vol. 56, no. 1, pp. 44-57, Mar. 2010.

[17] O. Soohyun, B. Kulapala, A.W. Richa and M. Reisslein, "Continuous-Time Collaborative Prefetching of Continuous Media," *IEEE Trans. on Broadcasting*, vol. 54, no. 1, pp. 36-52, Mar. 2008.

[18] O.T. Cruces, M. Fiore and J. M. B. Ordinas, "Cooperative Download in Vehicular Environments," *IEEE Trans. on Mobile Computing*, vol. 11, no. 4, pp. 663-678, Apr. 2012.

[19] V. Raveendran, P. Bhamidipati, X. Luo, X. Huang and C. Jia, "Mobile multipath cooperative network for real-time streaming," *Signal Processing: Image Communication*, vol. 27, no. 8, pp. 856-866, Sept. 2012.

[20] F. Malandrino, C. Casetti, C.-F. Chiasserini and M. Fiore, "Content Downloading in Vehicular Networks: What Really Matters," *Proc. IEEE*

International Conference on Computer Communications (INFOCOM), Apr. 2011.

[21] J. Zhao, P. Zhang, G. Cao and C.R. Das, "Cooperative Caching in Wireless P2P Networks: Design, Implementation, and Evaluation," *IEEE Trans. on Parallel and Distributed Systems*, vol. 21, no. 2, pp. 229-241, Feb. 2010.

[22] T. Do, K. Hua and N. Jiang, "PatchPeer: A scalable video-on-demand streaming system in hybrid wireless mobile peer-to-peer networks," *Peer-to-Peer Networking and Applications*, vol. 2, pp. 182-201, Feb. 2009.

[23] M. K. Denko, J. Tian, T. K. R. Nkwe and M. S. Obaidat, "Cluster-Based Cross-Layer Design for Cooperative Caching in Mobile Ad Hoc Networks," *IEEE Systems Journal*, vol. 3, no. 4, pp. 499-508, Dec. 2009.

[24] Yong Hao, Jin Tang and Yu Cheng, "Secure Cooperative Data Downloading in Vehicular Ad Hoc Networks," *IEEE Journal on Selected Areas in Communications/Supplement*, vol. 31, no. 9, pp. 523-537, Sept. 2013.

[25] B. Ahlgren, C. Dannewitz, C. Imbrenda, D. Kutscher and B. Ohlman, "A survey of information-centric networking," *IEEE Communications Magazine*, vol. 50, no. 7, pp. 26-36, July 2012.

[26] L. Blazevic, L. Buttyan and S. Capkun, "Self-Organization in Mobile Ad Hoc Networks: The Approach of Terminodes," *IEEE Communications Magazine*, vol. 39, no. 6, pp. 166-174, Apr. 2001.

[27] H. Lai, A. Ibrahim and K. J. R. Liu, "Wireless network cocast: location-aware cooperative communications with linear network coding," *IEEE Trans. on Wireless Communications*, vol. 8, no. 7, pp. 3844-3854, July 2009.

[28] C. Canali, M. E. Renda, P. Santi and S. Burresi, "Enabling Efficient Peer-to-Peer Resource Sharing in Wireless Mesh Networks," *IEEE Trans. on Mobile Computing*, vol. 9, no. 3, pp. 333-347, 2010.

[29] C. Fortuna and M. Mohorcica, "Trends in the development ofcommunication network: Cognitive networks," *Computer Network*, vol. 53, no. 25, pp. 1354-1376, June 2009.

[30] M. R. Bell, "Information theory and radar waveform design," *IEEE Trans. on Information Theory*, vol. 39, no. 5, pp. 1578-1597, Aug. 2002.

[31] Y. Bo and C.A. Balanis, "Least Square Method to Optimize the Coefficients of Complex Finite-Difference Space Stencils," *IEEE Antennas and Wireless Propagation Letters*, vol. 5, no. 1, pp. 450-453, Jan. 2006.

[32] D. P. Fogarty, A. L. Deering, S. Guo, Z. Wei, N. A. Kautz and S. A. Kandel, "Minimizing image-processing artifacts in scanning tunneling microscopy using linear-regression fitting," *Review of Scientific Instruments*, vol.77, no. 12, pp. 126104-126104-3, June 2006.

[33] V. Wong and V. Leung, "Location Management for Next-Generation Personal Communications Networks," *IEEE Network*, vol. 14, no. 5, pp. 18-24, Sept. 2000.

[34] J. Deng, "Grey linear programming," *International Conference Information Processing Management Uncertainty Knowledge-Based System*, 1986.

[35] J. Deng, "Introduction to grey system theory," *The Journal of grey system*, vol. 1, no. 1, pp. 1-24, 1989.

[36] C. Xu, F. Zhao, J. Guan, H. Zhang and G.-M. Muntean, "QoE-driven User-centric VoD Services in Urban Multi-homed P2P-based Vehicular Networks," *IEEE Trans. on Vehicular Technology*, vol. 62, no. 5, pp. 2273-2289, June 2013.

[37] A. Razzaq and A. Mehaoua, "Layered Video Transmission Using Wireless Path Diversity Based on Grey Relational Analysis," *Proc. of IEEE International Conference on Communications (ICC'11)*, May 2011.

[38] S.-B. Lee, G.-M. Muntean and A. F. Smeaton, "Performance-Aware Replication of Distributed Pre-Recorded IPTV Content," *IEEE Trans. on Broadcasting*, vol. 55, no. 2, pp. 516-526, June 2009.

[39] C. Xu, E. Fallon, Y. Qiao, L. Zhong and G.-M. Muntean, "Performance Evaluation of Multimedia Content Distribution Over Multihomed Wireless Networks," *IEEE Trans. on Broadcasting*, vol. 57, no. 2, pp. 204-215, June 2011.

[40] C. Xu, T. Liu, J. Guan, H. Zhang and G.-M. Muntean, "CMT-QA: Quality-aware Adaptive Concurrent Multipath Data Transfer in Heterogeneous Wireless Networks," *IEEE Trans. on Mobile Computing*, vol. 12, no. 11, pp. 2193-2205, Nov. 2013.

[41] C. Paasch, G. Detal, F. Duchene, C. Raiciu and O. Bonaventure, "Exploring Mobile/WiFi Handover with Multipath TCP," *ACM SIGCOMM Workshop on Cellular Networks*, Aug. 2012.

Shijie Jia received the M.S. degree from Kunming University of Science and Technology, Kunming, China in 2009. He is currently working toward the Ph.D. degree in the Institute of Network Technology, Beijing University of Posts and Telecommunications, Beijing, China. His research interests include next generation Internet technology, wireless communications and peer-to-peer networks.

Changqiao Xu received the Ph.D. degree from the Institute of Software, Chinese Academy of Sciences (ISCAS) in January 2009. He was an Assistant Research Fellow in ISCAS from 2002 to 2007, where he was a Research and Development Project Manager in the area of communication networks. During 2007 - 2009, he worked as a Researcher with the Software Research Institute at Athlone Institute of Technology, Athlone, Ireland. He joined Beijing University of Posts and Telecommunications (BUPT), Beijing, China, in December 2009, and was an Assistant Professor from 2009 to 2011. Currently, he is an Associate Professor with the Institute of Network Technology, and Vice-Director of the Next Generation Internet Technology Research Center at BUPT. He has published over 100 technical papers in prestigious international journals and conferences including IEEE transactions on mobile computing, IEEE transactions on vehicular technology, IEEE transactions on broadcasting, and Proceedings of ACM Multimedia. His research interests include wireless networking, multimedia communications, and next generation Internet technology.

Jianfeng Guan received his Ph.D. degrees in communications and information system from the Beijing Jiaotong University, Beijing, China, in Jan. 2010. He is a lecturer in the Institute of Network Technology at Beijing University of Posts and Telecommunications (BUPT), Beijing, China. His main research interests focus around mobile IP, mobile multicast and next generation Internet technology.

Hongke Zhang received his Ph.D. degrees in electrical and communication systems from the University of Electronic Science and Technology of China in 1992. From 1992 to 1994, he was a postdoctoral research associate at Beijing Jiaotong University (BJTU), and in July 1994, he became a professor there. He has published more than 150 research papers in the areas of communications, computer networks, and information theory. He is the author of eight books written in Chinese and the holder of more than 40 patents. He is the chief scientist of a National Basic Research Program ("973" program). He is Director of the Next Generation Internet Technology Research Center at Beijing University of Posts and Telecommunications (BUPT) and Director of the National Engineering Laboratory for Next Generation Internet Interconnection Devices at BJTU.
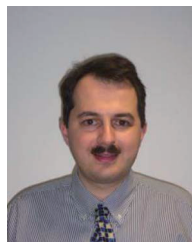
Gabriel-Miro Muntean received the Ph.D. degree from Dublin City University, Dublin, Ireland, for research in the area of quality-oriented adaptive multimedia streaming in 2003. He is a Senior Lecturer with the School of Electronic Engineering at Dublin City University (DCU), Dublin, Ireland. He is a Co-Director of the DCU Performance Engineering Laboratory, Director of the Network Innovations Centre, part of the Rince Institute Ireland and Consultant Professor with Beijing University of Posts and Telecommunications, China. His research interests include quality-oriented and performance-related issues of adaptive multimedia delivery, performance of wired and wireless communications, energy-aware networking, and personalized e-learning. He has published over 180 papers in prestigious international journals and conferences, has authored three books and 15 book chapters and has edited six other books. He is an Associate Editor of the IEEE transactions on broadcasting, Associate Editor of the IEEE communications surveys and tutorials, and reviewer for other important international journals, conferences, and funding agencies.